

Provided for non-commercial research and educational use only.  
Not for reproduction or distribution or commercial use.



This article was originally published in a journal published by Elsevier, and the attached copy is provided by Elsevier for the author's benefit and for the benefit of the author's institution, for non-commercial research and educational use including without limitation use in instruction at your institution, sending it to specific colleagues that you know, and providing a copy to your institution's administrator.

All other uses, reproduction and distribution, including without limitation commercial reprints, selling or licensing copies or access, or posting on open internet sites, your personal or institution's website or repository, are prohibited. For exceptions, permission may be sought for such use through Elsevier's permissions site at:

<http://www.elsevier.com/locate/permissionusematerial>

# Glory phenomenon informs of presence and phase state of liquid water in cold clouds

Anatoly N. Nevzorov

*Central Aerological Observatory, Dolgoprudny, Moscow Region, 141700, Russian Federation*

Accepted 12 January 2006

## Abstract

Although the optical phenomenon of glory on cloud tops with negative temperatures is now widely known to be observable from aircraft, the information thereby obtained on cloud microphysics remains not called for. The analysis made in the present work is based on a comparison between the features of the glory phenomenon, geometric theory of bow formation, and Mie scattering theory. The convincing evidence has been provided that this sort of glory forms as a first-order bow from spherical particles with a refractive index of 1.81–1.82 and diameter over 20  $\mu\text{m}$ . Thus obtained are solutions of two interrelated problems: (i) the cold-cloud glory is proved to be a bow formed from spheres with those unusual optical properties, (ii) once more corroboration is gained of earlier discovered existence in cold clouds of droplets of liquid water in specific phase state referred to amorphous water, or A-water. Physico-chemical and genetic peculiarities of A-water are briefly summarized here. The results obtained show that a detailed study and monitoring of the glory phenomenon are of great interest since the occurrences of the phenomenon itself as well as its geometrical and photo-chromatic characteristics provide unique remote information about the disperse phases of cold clouds. The visible size of the glory can serve as an indicator of the maximum size of A-water droplets, and its extra outer rings must reveal the presence of some forms of ice crystals.

© 2006 Elsevier B.V. All rights reserved.

*Keywords:* Cloud; Composition; Water; Phase; Bow

## 1. Introduction

The glory is classically defined as an optical phenomenon of an iridescent ring around the observer's antisolar shadow on a cloud or mist. It has long been referred to as Brocken specter that can occasionally appear on mountain mists. At present, the glory can be typically observed from an airplane (Fig. 1). Observations of it from space are now quite common as well.

To start with, it should be emphasized that the term "glory" is usually applied to backscattering effects that

are seemingly of the same nature, but quite different in their features. In this work, we consider the sort of glories that appear only on cloud (fog, mist) tops with temperatures below 0°C. To distinguish this phenomenon prior to discussing adequate terminology, let us conventionally call it "cold-cloud glory" (CCG). The case of cold clouds has been selected because despite the glory's being formed from spheres represented in clouds by liquid droplets, a number of specific problems connected with their liquid disperse phase remain unsolved. Unfortunately, information about the cold cloud liquid offered by CCG is still far from being well-understood and, therefore, from being called for in practice.

*E-mail address:* [an.nevzorov@mtu-net.ru](mailto:an.nevzorov@mtu-net.ru).



Fig. 1. The glory on the top of cold cloud around the airplane shadow. The center of glory ring identifies the camera location within the airplane.

Although today's demands and facilities make CCG both attractive and perfectly possible for careful study, no serious scientific interest in this phenomenon has actually been shown so far. No sufficiently objective, complete, and detailed description of the glory phenomenon can be found in literature that would throw light on the relation between its behavior and cloud properties. The following description relates to CCG only. It is based on the most representative description by Minnaert (1969), the observations of the author of this paper, and the analysis of about 30 color photographs of glories, made on diverse clouds from an airplane. The description is so framed as to discriminate diverse and seemingly unrelated features of the phenomenon:

- (i) The occurrence of multicolor glories on clouds with temperatures at their tops below  $0^{\circ}\text{C}$  is quite frequent if not typical, with clouds commonly referred to as purely ice ones included. We came across a number of cases when the glory could be seen within a transparent cloud, simultaneously with such ice-formed effects as the undersun and halo.
- (ii) The basic element of such a glory is a luminous and, as a rule, regular ring composed of color circles grading into each other. Its geometric center is located on the shadow projection of the observation point and is surrounded by a white aureole (Fig. 1).
- (iii) The radial sequence of colors in the glory ring always constitutes a red outer border grading into orange and yellow belts, and then to a more or less discolored interior part. The light throughout the

ring is strongly polarized positively, i.e. in the radial direction, as in a rainbow.

- (iv) In some cases, the basic ring is surrounded by one or more much weaker rings (Fig. 1) colored like basic one.
- (v) The angular radius of the basic ring belt close to yellow varies from case to case between  $1.5^{\circ}$  and  $3.8^{\circ}$ . The bigger the glory size, the brighter is its image.
- (vi) Both the visible size and brightness of the glory tend to increase as the cloud becomes more transparent. Conversely, the smallest, scarcely discernible and pale-colored glories generally occur in the densest clouds.

All the above features of the phenomenon can be easily confirmed through the simplest aircraft observations. The analysis of the CCG physical nature that follows builds upon the whole of features presented.

## 2. Physics of glory formation: versions and considerations

It is generally acknowledged that the glory phenomenon originates due to backscattering by spherical particles represented in clouds by water droplets. A certain disagreement takes place only about the physics of glory formation.

Formerly most popular idea of diffraction was strongly argued by van de Hulst (1957), and we cannot but accept his basic argument that the necessary condition for the diffraction effect, backward directed light originated within a cloud, is physically impossible. Later ideas follow a concept of backscattering corona formed by light scattered by individual droplet. The earliest study of the phenomenon, based on its laboratory modeling, took into account its intimate connection with a forth-scattering corona (Green and Lane, 1964). Early attempts to explain theoretically the physics of glory formation by droplets with refractive index  $n=1.33$  were undertaken by van de Hulst (1957) whose conclusions were deduced from laboratory results and far-fetched assumptions of speciality of small water droplets in optical properties.

At present, Mie scattering theory realized in computer programs represents an extremely powerful tool for calculation of any characteristics of light scattering by spheres of any size and optical properties. Such unique possibilities enabled a number of works devoted to seeking the proof of and clarifying the conditions for the appearance of peaks in the light scattered by water droplets ( $n=1.33$ ) at angles close to

180°, with the peaks considered to be forming a glory image. Remarkably, a common conclusion is that the real glory occurs only in clouds those consist of droplets of about 10 μm in size, as in turn next illustrated.

All our calculations below were performed by the Mie formulas using the universal computer program developed by Dr. A.G. Petrushin. As applied to an image formed at light scattering angle  $\beta > 90^\circ$  and observed from the side of light source, hereinafter the observation angle  $\varphi = (180^\circ - \beta)$  with an antisolar axis will be used as an angular parameter.

In Fig. 2, the angular functions are plotted of the intensity of light scattered by water droplets of different sizes at observation angles  $\varphi$  close to 0°. The calculations were made for two spectral bands, red one for liquid water  $n = 1.328$  for liquid water, and violet one ( $n = 1.340$ ). Each curve in Fig. 2 carries a peak with the angle of its top strongly depending on droplet size, so that the angle from 1.5° to 3.8° can result from nearly monodisperse droplets from  $\sim 8 \mu\text{m}$  to  $\sim 12 \mu\text{m}$  in diameter. The color sequence in the ring image follows that of CCG. However, along with this formal similarity, the calculations reveal a good number of substantial distinctions between the calculated “warm cloud” phenomenon and observed CCG:

- (i) The relation between the angle and the intensity of the peak formed at  $n \approx 1.33$  is opposite to that between the angular size and brightness of the basic CCG ring.
- (ii) A well-defined colored ring, like that of CCG in size, can be formed only by practically monodis-

perse droplets of strongly limited sizes, which is quite unlikely in nature. For real water clouds consisting of more or less polydisperse droplets, the effect proves to be fuzzy and manifests itself at best in a white ring, or most often in wide aureole, i.e. markedly differs from CCG.

- (iii) The theory for  $n \approx 1.33$  reveals no extra rings identical to regularly positioned, sequentially decaying rings episodically accompanying CCG. A number of calculated peaks in scattered light are smallest in relative height ( $\sim 1\%$ ), quite irregular and variable in angles depending on droplet size and light wavelength.
- (iv) The polarization efficiency in so calculated rings is always of negative sign in contrast with positive one as observed in CCG (all the calculated polarization data are quite uniform and thus are not shown graphically in the present paper).

So, even a cursory comparison leads to the conclusion that, in fact, we have to do with backscattering effects differing essentially in their features and, therefore, in the physics of their formation. This fact, among other things, makes us return to the problem of terminology. Reasoning from the classical definition of the glory phenomenon given in textbooks and followed by van de Hulst (1957), Minnaert (1969), and the above description, the term “glory” would be equitably applied only to CCG. As to the other sort of the phenomenon, inherent only in purely water, mainly warm clouds, it can be called by its original alternative name “back (or backscattering) corona”. To avoid ambiguity, hereinafter

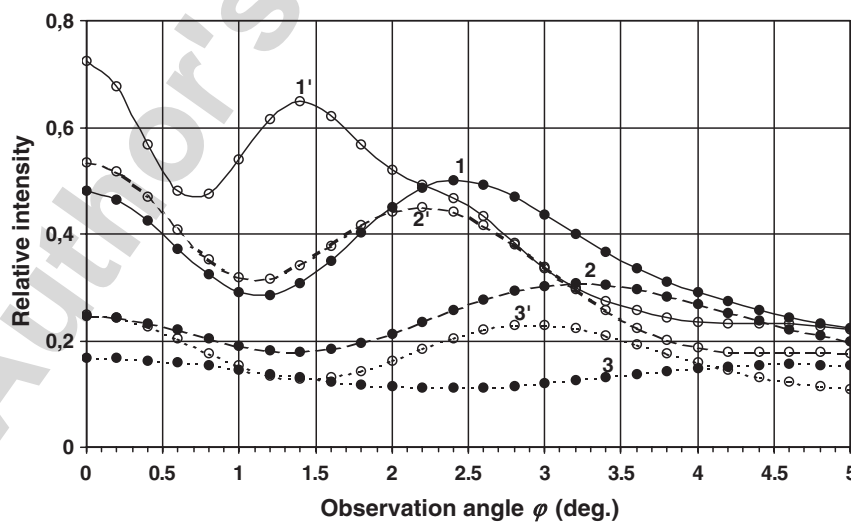


Fig. 2. Angular functions of the relative intensity of light back scattered by water droplets of 12 μm (1, 1'), 9 μm (2, 2'), and 6 μm (3, 3') in diameter, calculated by Mie theory: 1, 2, 3—for  $n = 1.328$  in red spectral band ( $\lambda = 0.67 \mu\text{m}$ ), 1', 2', 3'—for  $n = 1.340$  in violet band ( $\lambda = 0.42 \mu\text{m}$ ). The functions are normalized to the droplet cross-section unity. The peak of each curve defines an element of the backscattering corona from a water cloud. It can be seen that the corona becomes more distinct and brighter with its visible size diminishing, while the natural glory exhibits an inverse dependence.



we will follow this terminology. In addition to the differences listed above, the backscattering corona with its features yields to the prediction by Mie theory, while the classical glory still resists a similar solution. To all appearances, a back corona is akin to a forth corona in resonance or diffraction nature. At the same time, the glory phenomenon as described above is yet lacking in any plausible explanation.

The idea of the glory to be a scattering bow has never been seriously considered due to the old-proven (van de Hulst, 1957) impossibility for a bow, if formed by water ( $n \sim 1.33$ ) or ice ( $n \sim 1.31$ ) spheres, to have such a small visible angle. Instead, a rainbow having the angle of  $\sim 42^\circ$  is readily detectable with the Mie tools. Nevertheless, there are reasons to accept the bow concept in our case as well.

### 3. The glory as a bow

#### 3.1. General remarks

The commonly known phenomenon of crystal riming in clouds (e.g. Pruppacher and Klett, 1978) as well as recent aircraft measurements (Cober et al., 1996; Mazin et al., 1992) have evidenced that liquid droplets reaching tens to hundreds of micrometers in diameter are typically present in ice-containing cold clouds. Nevzorov (1992, 1993, 2000) has received preliminary experimental result that the refractive index of a substance of such droplets lies between 1.8 and 1.9 in visible light, and has come to the conclusion that they consist of water in a specific amorphous phase, or A-water. The idea of the glory origination as a bow formed in the light scattered from this kind of particles, capable of existing only at negative temperatures, is in full agreement with the first item of the above description.

The bow's visual image is formed in the observer's eye by rays of light scattered by a mass population of space-dissipated spherical particles, such as liquid or frozen droplets. Since the converging rays forming the bow issue from an individual sphere at a definite angle along a cone generatrix, the rays radiated from an assemblage of such particles reach the observer at the vertex of an inverse cone with the same angle as shown in Fig. 3, thus creating a circular image. In reality, only bows formed near cloud tops in reflected sunlight can be distinctly observable as in Fig. 1; otherwise, the rays creating the image will be vastly scattered in a bulk of cloud body.

There are two approaches to theoretical describing bow behavior. These are an approximate geometric theory and a rigorous Mie theory. A comparison

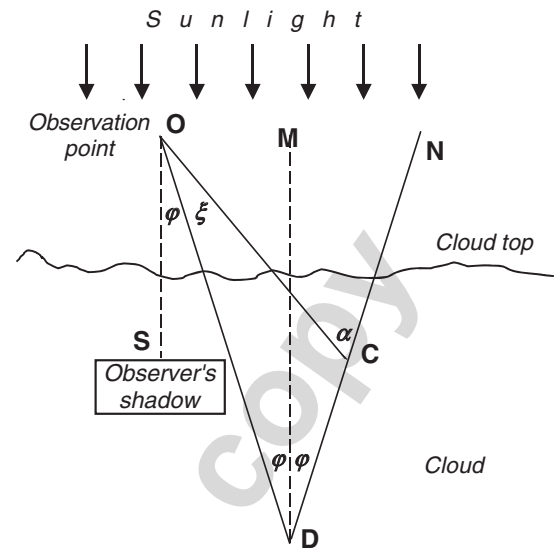


Fig. 3. Schematic two-dimensional diagram of the formation of glory image with the first secondary ring. The straight lines **OS** and **MD** are sunlight rays, **DO** and **DN** are the bow rays emitted by droplets located at point **D** so that the **DO** ray penetrates the observer's eye at angle  $\varphi$  with the bow axis **OS**. Here  $\varphi = \pi - \beta$ , where  $\beta$  is the scattering angle. The line **CO** is the ray formed presumably by ice crystals from the bow ray **DN** at the halo angle,  $\alpha$ , as discussed in Section 4.

between the results of the two independent theories as well as between them and the properties of a real glory (CCG) will offer a criterion of the validity of the suggested interpretation of its physical nature.

#### 3.2. Geometric theory

The geometric theory of the bow is based on the analysis of the ray paths within an individual transparent sphere with refractive index  $n$ , illuminated by a parallel light beam (e.g. Shifrin, 1983). The bow is defined as a product of the convergence of rays reflected from the interior spherical surface and then leaving the sphere after  $k \geq 1$  reflections. The total angle of the turn of the rays forming  $k$ -order bow can be expressed as

$$\gamma^{(k)}(n) = k\pi + 2\arcsin \frac{A}{n} - 2(k+1)\arcsin A, \quad (1)$$

where

$$A = \sqrt{\frac{(k^2 + 1)^2 - n^2}{k^2 - 1}}. \quad (2)$$

These rays leave a particle at scattering angle

$$\beta^{(k)} = |\gamma^{(k)} - 2\pi j|, \quad (3)$$

where  $j \geq 0$  is an integer providing the condition  $0 < \beta^{(k)} < \pi$ . In the case of  $\pi/2 < \beta^{(k)} < \pi$  referring to

backscattering bow like familiar rainbow, its visible, or observation angle from the observer's eye is

$$\varphi^{(k)} = \pi - \beta^{(k)} < \pi/2. \quad (4)$$

Fig. 4 shows calculated from Eqs. (1)–(4) dependence of observation angles  $\varphi < 70^\circ$  of backscattering bows of orders of 1 to 7 upon the refractive index  $n$  of scattering spheres. Quite apparently, the bow intensity rapidly decreases with its order increasing, and so the graphs for the bows of higher orders are here omitted. The dependence  $n(\lambda)$ , where  $\lambda$  is the light wavelength, results in the dependence  $\varphi^{(k)}(\lambda)$ , thereby, in the color palette of bows of every order. Since the value of  $n$  for water increases from red to violet edge of the visible light spectrum, an elementary bow related to a drop-down curve in Fig. 4 has its red belt from outside, and vice versa.

To make sure of the validity of the geometrical approach, note that at  $n \approx 1.33$  both the number and angle domain of thus modeled elementary bows of different orders closely follow those of must complete image of the natural rainbow. Fig. 4 clearly demonstrates that the latter consists of four elementary bows of the orders 1 (with  $\sim 42^\circ$  angle), 2, 5, and 6.

Turning to the glory with its observation angle between  $1.5^\circ$  and  $3.8^\circ$ , one might assume from Fig. 4 that this could be, for example, 5-order bow from droplets with  $n \sim 1.43$ . However, the same diagram requires that any backscattering bow of over first order be combined with first order bow. In the given case, this well brighter bow must be of  $\sim 30^\circ$  angle. At the same time, no iridescent ring other than ones close to  $42^\circ$  (rainbow) and  $3^\circ$  (glory) occurs in natural clouds at all.

It only remains to conclude that the basic ring of the glory is the first order bow formed by spherical particles which refractive index  $n$  is close to 1.8.

The shortcomings of the geometric approach here presented are: (i) ignoring scattering particles size responsible for the difference between the wave phases of interfering rays, which results in non-adequate determination of the angles of elementary bows, and (ii) an utter absence of the information of intensity, angular profile and polarization of an elementary bow. Mie theory rigorously allows for these factors.

### 3.3. Mie approach

To demonstrate the effectiveness of the Mie tools in the bow prediction, let us again refer to the example of common rainbow. Fig. 5 represents the calculated angular functions,  $I(\varphi)$ , of the intensity of light scattered by droplets of ordinary water with  $d=150\mu\text{m}$  in red spectral band ( $n=1.328$ ) and in yellow one ( $n=1.334$ ). The curves exhibit four distinct peaks obviously corresponding to four bows of different orders just as mapped in Fig. 4. To aid in the identification of their orders in Fig. 5, the angle sequences of neighbor peaks belonging to curves for different  $n$  have been related to the derivative sign of the corresponding curve in Fig. 4. It can be seen that the difference between the bow angles determined geometrically and by Mie theory increasingly grows with the bow order. Besides (not shown here), as droplet size decreases, this difference additionally increases and the peaks become lower and wider. The calculated polarization of light within the rainbow domain is of positive sign and closely correlates with the peaks.

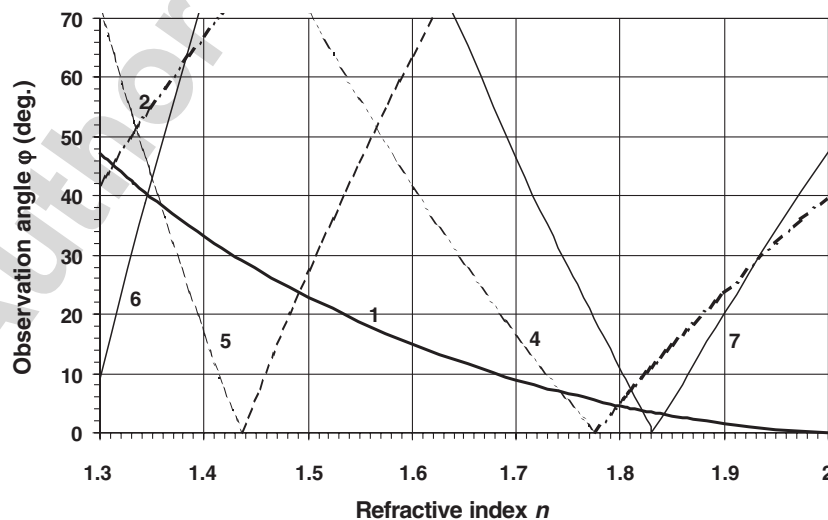


Fig. 4. A set of observation angles  $\varphi^{(k)}$  for backscattering bows of different orders  $k \leq 10$  versus refractive index  $n$  of scattering spherical particles, calculated from the geometric theory irrespective of particle size.

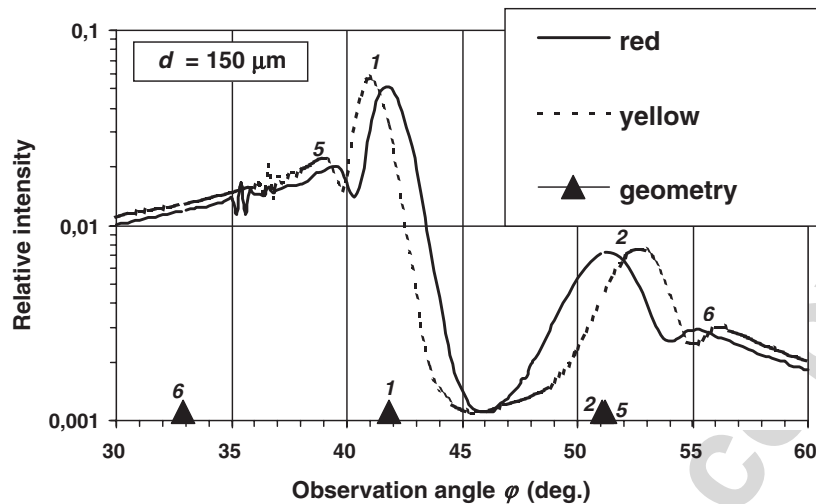


Fig. 5. Angular functions of the scattering intensity of water droplets with  $d=150\ \mu\text{m}$  over the angle domain of the natural rainbow, calculated by Mie formulas at  $n=1.328$  for the red spectral band ( $\lambda=0.67\ \mu\text{m}$ ) and at  $n=1.334$  for yellow one ( $\lambda=0.58\ \mu\text{m}$ ). The numbers by the peaks denote the bow's order. For comparison, at the bottom diagram the angles are shown of the bows of the corresponding orders, calculated from the geometric theory at  $n=1.334$ .

Now let us examine the glory angle domain. Fig. 6 gives the notion of the 1-order bow behavior depending on sizes of scattering spheres with  $n=1.81$ . With  $d$  increasing, the peak in the corresponding curve arises at almost  $20^\circ$  and then becomes higher and narrower, the angle of its top,  $\varphi_m(n,d)$ , approaching that in Fig. 4. Not more than one distinct peak is found in each curve at  $\varphi < 90^\circ$ . The calculations revealed positive peaks of polarization efficiency exactly coinciding with the peaks of light scattering intensity. All this, together with the graph in Fig. 4, implies that the resulting peaks in graphs of Fig. 6 are indications of the first order bow produced by particles of different sizes.

How the bow angle depends on the refractive index  $n$  at different droplet sizes, has been derived from the set of curves  $I(n,\varphi)$  like as plotted in Fig. 6, and is shown in Fig. 7. Also presented here is the “geometric” curve  $\varphi^{(1)}(n)$  obtained irrespective of  $d$ . Fig. 8 graphically demonstrates that the “geometric” curve in Fig. 7 is the locus of asymptotes of the peak angles at different  $n$  with  $d \rightarrow \infty$ .

Thus, we have sufficient reason to conclude that the glory (by its classical definition) is physically a bow formed by large enough spheres whose reflective index is much larger than that of ordinary water. Such spheres in cold clouds can be only droplets consisting of A-water.

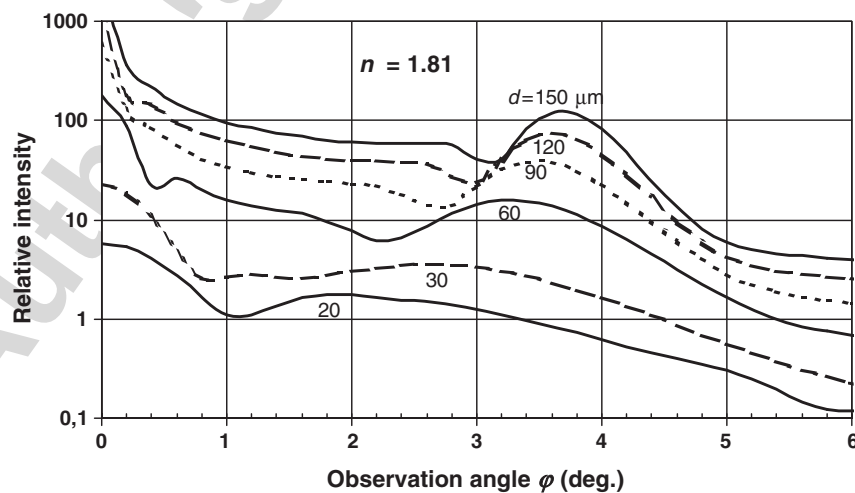


Fig. 6. The angular functions of scattering intensity calculated from the Mie formulas at  $n=1.81$  and  $\lambda=0.58\ \mu\text{m}$  (yellow light) over the angle range wherein the intensity peaks occur at different diameters,  $d$ , of scattering spheres. The data are normalized to the unit of the cross-section of scattering spheres. The relationship between the visible size and the sharpness as well as the brightness of the ring's image thus formed is opposite to that in Fig. 1 and corresponds to the behavior of natural glory.

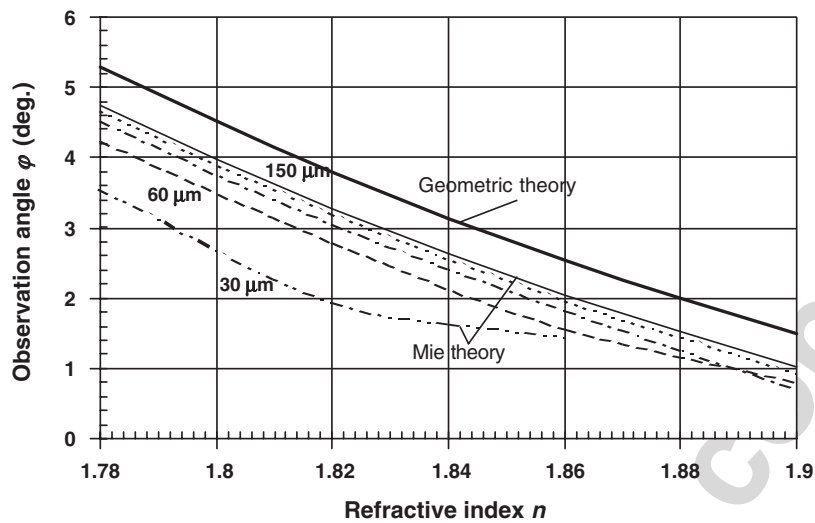


Fig. 7. Bow angle  $\varphi^{(1)}$  versus refractive index  $n$  derived from Mie theory for sphere diameters 30 (30) 150  $\mu\text{m}$  at  $\lambda=0.58\mu\text{m}$  (yellow light), and calculated for comparison by geometric theory.

The Mie theory affirms that both brightness and color contrast of the glory directly depend on the size of scattering droplets. It can be seen from Fig. 6 that the most luminous and highly colored glories are formed by droplets larger than 150  $\mu\text{m}$ . That such droplets can really occur in cold clouds was certified by Cober et al. (1996) who reported on freezing drizzle droplets reaching almost 0.5 mm in diameter.

Considering all the above, one can infer from Fig. 7 that natural glories seen at a  $1.5^\circ$  to  $3.8^\circ$  radial angle of the yellow belt are produced by spheres larger than  $\sim 20\mu\text{m}$  in diameter, which refractive index lies between 1.81 and 1.82 for the yellow spectral band.

The shape of each peak in Fig. 6 reproduces the ring width of the bow formed by monodisperse droplets

illuminated by monochromatic light. The total width of the ring of real glory is mainly determined by the droplet size spectrum. In case of a wide enough spectrum, different colors are mixed within the ring so that its larger part, other than the red outer edge, can look either almost or completely discolored. Besides, one can see from Fig. 6 that the central aureole is always, just as in reality, present in the glory picture, with its width rather weakly depending on droplet size.

The angular functions of scattering intensity plotted in Fig. 9 were calculated for  $d=150\mu\text{m}$  at two values of the droplet refractive index. Here  $n=1.81$  approximately corresponds to yellow light for A-water, and  $n=1.79$  is chosen based on the ratio of both peak angles being close to that of the sizes of the red and

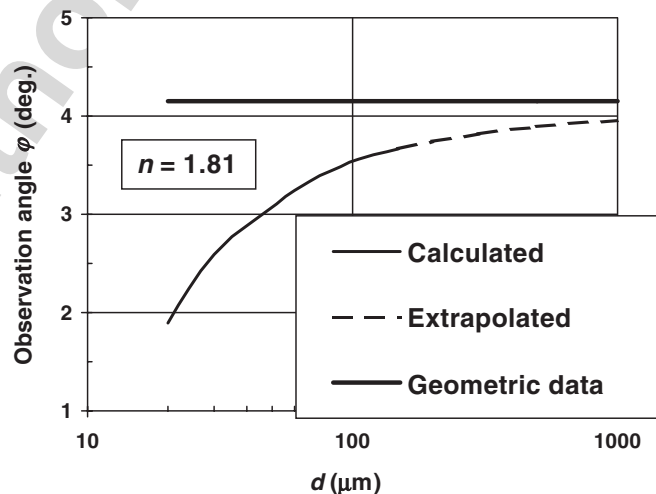


Fig. 8. An illustration of the “geometric” curve in Fig. 7 being the locus of the Mie curve at  $d \rightarrow \infty$ .



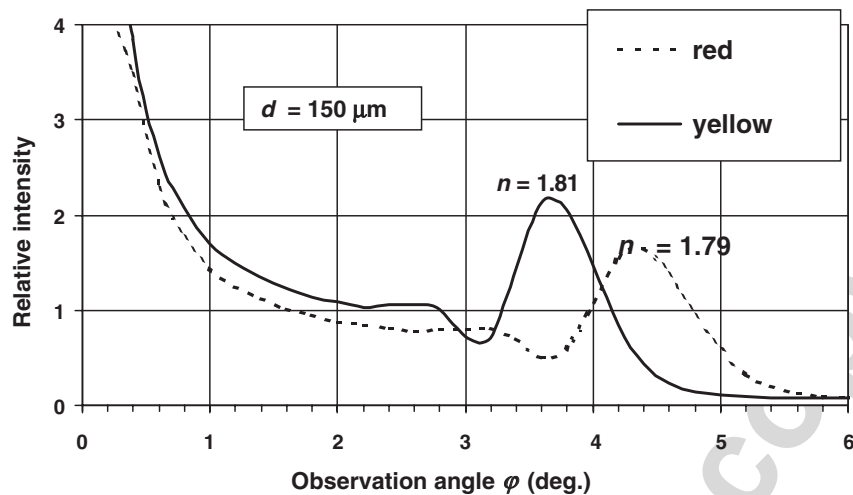


Fig. 9. The ratio of sizes of the glory's red and yellow belts enabled to estimate the difference between A-water refractive indexes in the corresponding spectral bands. Details are in the text.

yellow belts of a real glory. Hence, in the red spectral band, A-water has  $n \approx 1.79 \div 1.8$ . Therefore, its color dispersion is expected to be much more appreciable than that of ordinary water.

#### 4. On the extra rings and forward scattering bows

As mentioned above, all the attempts failed to find any sign of higher-order bows surrounding the first order bow that constitutes the basic ring of a glory. This is probably due to their peaks at  $d \leq 150 \mu\text{m}$  being extremely small or so displaced from their position in Fig. 4 that they practically merge either with the central aureole or with the 1-order bow. The essentially equidistant rings episodically accompanying real glories are far out of expected properties of 4- and 7-order bows formed by substantially bigger droplets. Nothing remains for us here but to consider such extra rings as resulting from secondary scattering in a cloud. We cannot point to some mechanism of scattering from spherical droplets that could result in the said effect. On the other hand, there are reasons to postulate that such extra rings are produced by ice crystals.

The scheme of formation of the first of secondary rings is presented in Fig. 3. Besides the bow's direct ray **DO** formed in droplets at scattering angle  $\beta$  and observed at angle  $\varphi = \pi - \beta$ , secondary rays are coming to the observer scattered by cloud particles from the diametrically symmetrical ray **DN** of the same bow. The visible ring stands out against the background-scattered light due to the peak of scattering intensity at angle  $\alpha$  inherent in ice crystals of a certain type. Such peaks are responsible for the formation of haloes of different

angular sizes (Minnaert, 1969; Volkovitsky et al., 1984). As can be seen from Fig. 3, the angle **DOC** between the basic and extra rings is  $\xi = \alpha - 2\varphi$ , whence the radial angle **COS** of the extra ring is

$$\varphi_1 = \xi + \varphi = \alpha - \varphi. \quad (5)$$

The corresponding halo angle can be readily determined from direct angular measurements as

$$\alpha = 2\varphi + \xi. \quad (6)$$

By estimations, the  $\alpha$  value for the first extra ring is kept distinctly constant at  $8.5^\circ \div 9^\circ$ . This result reasonably coincides with the peak angle responsible for a so-called Van Buijsen halo peculiar to some pyramid-like crystal forms (Volkovitsky et al., 1984). However, subsequent rings lack similar relations with known halo angles. They might result either from specific crystal types, perhaps most common to a cloud top, or due to consecutive re-scattering steps. In any case, their origin needs to be yet understood.

Finally, it should be noted that, as calculated from Eqs. (1)–(3), at  $n \approx 1.81 \div 1.82$  all forward directed bows of orders 2, 3, 5, 6, 8 and 9 are concentrated between the scattering angles,  $\beta$ , of  $\sim 40^\circ$  and  $\sim 70^\circ$ . We believe that such bows, most possible of 2nd and 3rd orders, are responsible for the effect of spot irisation of high cloud edges illuminated by sunlight, as can occasionally be seen from the ground.

#### 5. On some properties and nature of A-water

The offered interpretation of the glory phenomenon, on the one hand, fully conforms to its behavior when

appearing on natural *cold* clouds, and on the other hand, provides independent corroboration of presence in such clouds of large enough spherical particles with as high refractive index as 1.8 or somewhat more, as found earlier by Nevzorov (1992, 1993). As previously, we find no other realistic explanation of a nature of those particles than liquid droplets consisting of a specific state of water represented by amorphous, or A-water. This yet little known water phase has been first produced and investigated in laboratory as solid and viscose glassy state at temperatures as low as 100...150 K (Delsemme and Wenger, 1970; Skripov and Koverda, 1984). This kind of works was in time growing in amount as surveyed in details by Skripov and Koverda (1984) and Angell (2004). The laboratory examinations revealed two kinds of amorphous water, namely of high and of low density (Angell, 2004), but no satisfactorily valid result has been produced of even routine properties as well as comparative interior structures of these two modifications, if any. No evidence was offered by laboratory facilities of existence and behavior of the amorphous water at temperatures up to 0°C, much less at higher ones. It turns out that atmospheric clouds can serve as a ready natural plant for producing purest, long-lived, wide-temperature liquid amorphous water to be thoroughly investigated. The glory phenomenon proves that the cloud A-water is water modification of the highest density as earlier measured by Delsemme and Wenger (1970).

The typical appearance of glory in cold, especially ice-containing clouds must signify that they as a rule, if not always, contain A-water droplets from ~20 to hundreds micrometers in diameter. We have made sure from the glory behavior that the more transparent (and therefore, recognized as purely ice) is a cloud, the bigger are the droplets therein. This once again suggests that A-water droplets can experience condensation growth in the permanent presence of ice particles, which implies the existence of condensation equilibrium between A-water and crystalline ice.

*Can air suspended droplets of A-water exist at positive temperatures?* Rather obviously, this is in principle impossible for the following reason. While the temperature curve of saturated vapor pressure over ordinary liquid water keeps smooth at any temperature, like curve for ice and, equivalently, for A-water connects it at 0°C at a nonzero angle from below. Thus, the mere smooth extrapolation of the “ice” curve shows that at  $T > 0^\circ\text{C}$  the A-water saturation vapor pressure becomes higher than that of ordinary water, and therefore is unattainable in real atmospheric air where

either condensation nucleus or droplets of ordinary water are of common presence.

The analysis above has aided in considerably specifying such a physical attribute of A-water as its refractive index. As compared with the previous rough estimation of  $n \approx 1.8 \div 1.9$ , the newly obtained result is  $n \approx 1.81 \div 1.82$  for yellow light. From Lorenz–Lorentz formula interrelating refraction index  $n$  and density  $\rho$  with sufficient accuracy for water (Eisenberg and Kauzmann, 1969):

$$\rho = \frac{1}{P(\lambda)} \frac{n^2 - 1}{n^2 + 2} \quad (7)$$

where  $P(\lambda)$  is specific refraction of  $0.206 \text{ dm}^3/\text{kg}$  for yellow light, we find A-water density  $\rho_A \approx 2.1 \text{ kg dm}^{-3}$ . A similar value  $2.32 \pm 0.17 \text{ kg dm}^{-3}$  has been obtained by Delsemme and Wenger (1970) from measurements of volume and mass of amorphous ice condensed at ~100 K. The amorphous condensate is found to transform from solid to viscous state when heated to 135 K and to acquire fluidity (becoming liquid) at ~150 K (Skripov and Koverda, 1984; Smith and Kay, 1999). All like considerations give grounds to identify in-cloud A-water and the known amorphous ice (sometimes referred to as A-ice) as two different aggregative states of the same water phase, A-water being melted A-ice. (Compare this with solid and melted glass. Note that ordinary liquid water and crystalline ice represent *different phase states* of water.) Experimentally, the melt of amorphous ice, that is A-water, can form directly through vapor condensation, as amorphous ice does, and spontaneously makes the transition to crystalline ice-I as opposed to solid A-ice.

As distinct from ordinary water and ice, the amorphous water/ice is lacking in the intermolecular hydrogen bonds. Its superhigh density results from hydrogen bonds keeping the molecules farther apart as compared with other bonds inherent to simple liquids. This can even be seen from the fact that crystalline ice with its completely realized hydrogen bonds is less dense than ordinary liquid water with a part of hydrogen bonds broken.

The physical properties of A-water discovered to date are listed in Table 1.

The crucial question about the nature of A-water and its place in the chain of water phase transitions has been discussed by Nevzorov (2000) and is to be briefly summarized here.

With its internal energy being the highest among all condensed phases of water, A-water is capable of originating adiabatically only from vapor condensation.

Table 1  
Experimentally determined physical properties of amorphous water

Property	Characterization	Condition	Notes
Vitrification/softening temperature	135 ± 1 K	$\eta = 10^{12} \text{ N s m}^{-2}$	1
Fluidity limit temperature	~ 150 K	$\eta = 10^8 \div 10^9 \text{ N s m}^{-2}$	1
Dynamic viscosity, $\eta$	$< 10^{-2} \text{ N s m}^{-2}$	$T > 218 \text{ K}$	1,2
Density	2.3 kg dm <sup>-3</sup>	Solid state, $T \approx 100 \text{ K}$	3
	2.1 kg dm <sup>-3</sup>	Liquid state, tropospheric clouds	4
Specific heat of evaporation	$0.55 \times 10^6 \text{ J kg}^{-1} \pm 20\%$	$T = 243 \text{ K}$	5
Latent heat of crystallization to ice I	$2.29 \times 10^6 \text{ J kg}^{-1} \pm 5\%$	$T = 243 \text{ K}$	6
Optical form	Transparent, colorless		1
Refractive index	1.79 ÷ 1.8	Red light	7
	1.81 ÷ 1.82	Yellow light	
Partial pressure of saturated vapor	The same as that of ice I	$T < 273 \text{ K}$	5

Notes:

1. By Skripov and Koverda (1984).
2. Estimated from the extrapolation of the experimental dependence  $\eta(T)$ .
3. By Delsemme and Wenger (1970).
4. Calculated from the refractive index by Lorenz–Lorentz formula (7).
5. By Nevzorov (1992, 1993).
6. Determined as the difference between the evaporation heat amounts for crystalline ice I and A-water.
7. This paper.

Like supercooled ordinary water, A-water can crystallize into ice-I (i.e. freeze) when in contact with ice-forming nuclei (IFN). However, in contrast to ordinary water, the probability of A-water crystallization increases with temperature (Skripov and Koverda, 1984). By all evidence, it is just A-water that constitutes an “intermediate step” phase in the vapor-to-ice transition in accordance with Ostwald’s rule. In the absence of IFN, A-water can remain in metastable state, thus forming liquid droplets in cold clouds. The aforementioned condensation equilibrium between A-water droplets and ice crystals implies that so-called “quasi-liquid” surface layer on ice particles (Jellinek, 1967) actually consists of amorphous water, as suggested by Fletcher (1970). (Note that mutual insolubility of A-water and ordinary water as well as the difference in their refractive indexes make it possible to observe, under intensive side illumination, the residuals of that “quasi-liquid” film during the process of melting of ice in a glass vessel. The resulting “flakes” of A-water slowly descend to the vessel bottom, accidentally merging while descending, and disperse again when the water is stirred up).

The steady coexistence of free A-water with cloud ice implies that the processes of condensation and partial crystallization of A-water droplets play a significant role in the formation of cloud phase composition. As for A-water condensation nuclei (AWCN), the abundance of atmospheric layers free of clouds at ice supersaturation signifies that no such active nuclei are generally present in dry air. One at least of the mechanisms of their natural

initiation is indirectly indicated by Rosinski and Morgan (1991), who found that a supercooled water droplet just evaporated could be immediately replaced by a newly formed ice crystal. In fact, as follows from the foregoing, the dehydrated residuals of ordinary water droplets acquire the properties of the catalytic centers of A-water condensation, and only part of them those of A-water crystallization centers. Such secondary AWCN can be collectively generated within a supercooled water cloud when relative humidity lowers sufficiently for the smallest droplets to evaporate. This process may occur near cloud edges, or due to dry air entrainment, or as a finale of the cycle of wetting non-hygroscopic nuclei, etc. In any case, both A-water droplets and ice crystals will originate in a cloud of supercooled ordinary water most probably at the very beginning of its lifetime (Nevzorov and Shugaev, 1992; Nevzorov, 1996). Both kinds of particles grow together through Bergeron–Findeisen process. Simultaneously, droplets of ordinary water evaporate so that the cloud remains mixed in phase, though acquiring abnormally large drops of A-water instead of ordinary water droplets typical in size of purely water clouds. All this determines that *A-water droplets serve as an attribute of not simply cold clouds but of ice-containing ones.*

## 6. Discussion and conclusions

Strangely enough, such readily available phenomenon as iridescent glory occurring around antisolar shadow of a plane or satellite on cold, mainly ice-

containing clouds has attracted so little attention of cloud physicists. The point is that this phenomenon is known to originate optically only in spherical particles, and therefore carries objective information, at least, of liquid (or assumed frozen) droplets in a cloud. The added complication is that the glory appears in practically all cases of ice-containing clouds and even down to temperatures beneath  $-40^{\circ}\text{C}$ , which can be easily verified by everyone though yet remains difficult to explain from the current knowledge. Evidently, the most realistic of various versions consists in specific state and peculiar properties of water forming those droplets, inasmuch as the possibility of existing of unusual in properties water at negative temperatures have been earlier discovered not only in laboratory experiments but also in cloud microphysical research.

Calculations of scattering indicatrices made here by Mie theory resulted in that the scattering peaks within the angle domain corresponding to the range of visible sizes of natural glory ( $1.5^{\circ}$  to  $3.8^{\circ}$  in radius of its yellow belt) can be of two kinds of their origin. In case of ordinary liquid water with refractive index  $n \approx 1.33$ , this is backscattering corona from droplets of 8 to  $12\mu\text{m}$  in diameter. There is the other case when these peaks appear when  $n = 1.81 \div 1.82$  and scattering spheres are larger than  $\sim 20\mu\text{m}$  up to unlimited size. From the comparison with independent geometric approach, it was concluded that the second solution represents a scattering bow of the first order formed by real spheres of corresponding properties, just as well-known rainbow is produced by the drops of ordinary water.

The physical interpretation of these theoretical results was based on the following grounds:

- (i) As distinct from the backscattering corona, the calculated model of bow follows natural glory in every detail of its behavior;
- (ii) Big size and high refractivity theoretically predicted for the dissipating spheres fit wholly in the results of complex microphysical measurements made earlier in ice-containing clouds (Nevzorov, 1992, 1997);
- (iii) No substance but practically pure water can constitute cloud spheres possessing such unusual properties.

All this allows inferring that the following interrelated principal results have been here achieved:

- The optical phenomenon of glory on cold clouds has been proved to be a bow formed from sunlight

scattering by spherical particles over  $\sim 20\mu\text{m}$  in size, with a refractive index of  $1.81 \div 1.82$  in yellow light,

- Extra corroboration is thereby gained of the existence in ice-containing clouds of droplets of liquid water in a specific phase state referred to as amorphous water, or A-water.

The results obtained suggest that the glory phenomenon should attract the attention of cloud physicists to be thoroughly investigated. The appearance, as such, of distinct iridescent ring of glory in a cold cloud implies that it contains liquid disperse phase in the form of A-water droplets. The angular size and width of the ring as well as its photometric and chromatic characteristics carry unique remote information on the size spectrum and concentration of A-water droplets. Finally, outer extra rings in the whole glory picture are most probably indicative of the presence in the cloud of ice crystals of a particular type.

It is significant that the independent corroboration of existence of A-water in cold clouds turns its hypothetical, as if, status to reality. We consider however that the most convincing confirmation of the conception of cloud A-water is in that it represents universal clue to understanding yet unsolved problems of the physics of cold clouds. These are anomalous stability of mixed phase composition of layer-type clouds, superhigh concentration of cloud crystals in comparison with that of detectable ice forming nuclei, origin of so-called supercooled rain or “freezing drizzle”, or of mixed precipitation, and other hardly explainable phenomena involved.

We are sure that the A-water conception must make up utterly lacking link in the current knowledge of cold clouds and thus is worthy of further investigation. In particular, it must radically change the current understanding of the energetics of cloud phase transformations. The fact that the specific heat of A-water evaporation is approximately five times less than that of ordinary water leads to the corresponding underestimation of conventional ‘hot wire’ measurements of liquid water content in mixed clouds. With the permanent presence of A-water in cold, even in seemingly ice clouds, its total mass in atmospheric clouds turns out to be many times that assumed by the existing concepts for the ordinary water. It follows from Table 1 that when freezing, A-water evolves about seven times as much energy as the same mass of ordinary water. Thus, there is every reason to suggest that the mass freezing of cloud A-water is quite possible source of almost two orders greater, than expected, energy of



destructive processes associated with clouds, from local tornado to global-scale hurricane.

It is easy to conjecture that the spherical particles discovered optically in stratospheric clouds as well as in cold cloudiness of some other planets can actually be A-water droplets.

### Acknowledgements

The author is grateful to Dr. Alexander Petrushin for his universal and handy computer program provided for the Mie calculations, and to Dr. Alexei Korolev for his critical discussion on the problem as well as for his representative collection of glory photographs taken from airplane.

### References

- Angell, C.A., 2004. Amorphous water. *Annu. Rev. Phys. Chem.* 55, 559–583.
- Cober, S.G., Strapp, J.W., Isaac, G.A., 1996. A case study of freezing drizzle formed through a collision coalescence process. *J. Appl. Meteorol.* 35, 2250–2260.
- Delsemme, A.H., Wenger, A., 1970. Superdense water ice. *Science* 167, 44–45.
- Eisenberg, D., Kauzmann, W., 1969. *The Structure and Properties of Water*. Oxford Univ. Press, Oxford.
- Fletcher, N.H., 1970. *The Chemical Physics of Ice*. Cambridge Univ. Press.
- Green, H., Lane, W., 1964. *Particular Clouds: Dusts, Smokes and Mists*, 2nd ed. Van Nostrand Co., London. 420 pp.
- Jellinek, H.H.G., 1967. Liquid-like (transition) layer on ice. *J. Colloid and Interface Sci.* 25 (2), 192–197.
- Mazin, I.P., Nevzorov, A.N., Shugaev, V.F., Korolev, A.V., 1992. Phase structure of stratiform clouds. 11th Int. Conf. on Clouds and Precipitation, Montreal, Canada, pp. 332–335.
- Minnaert, M., 1969. *Light and Color in the Nature*. Nauka, Moscow. 344 pp. (in Russian, translated from English).
- Nevzorov, A.N., 1992. Permanence, properties and nature of liquid phase in ice-containing clouds. 11th Int. Conf. on Clouds and Precipitation, Montreal, pp. 270–273.
- Nevzorov, A.N., 1993. Studies into the physics of liquid phase in ice-containing clouds. *Meteorol. Gidrol.* (1), 55–68 (in Russian).
- Nevzorov, A.N., 1996. Observations of initial stage of ice development in supercooled clouds. 12th Int. Conf. on Clouds and Precipitation, Zurich, pp. 124–127.
- Nevzorov, A.N., 1997. An experience and promising results of advanced measurements into microphysics of cold clouds. WMO Workshop on Measurements of Cloud Properties for Forecasts of Weather and Climate, Mexico, pp. 173–182.
- Nevzorov, A.N., 2000. Cloud phase composition and phase evolution as deduced from experimental evidence and physico-chemical concepts. 13th Int. Conf. on Clouds and Precipitation, Reno, Nevada, USA, pp. 728–731.
- Nevzorov, A.N., Shugaev, V.F., 1992. Observations of the initial stage of evolution of ice phase in supercooled clouds. *Meteorol. Gidrol.* (1), 84–92 (in Russian).
- Pruppacher, H.R., Klett, J.D., 1978. *Microphysics of Clouds and Precipitation*. D. Reidel Publ. Co. 714 pp.
- Rosinski, J., Morgan, G., 1991. Cloud condensation nuclei as a source of ice-formation nuclei in clouds. *J. Aerosol Sci.* 22 (2), 123–133.
- Shifrin, K.S., 1983. *Introduction to the Ocean Optics*. Gidrometeoizdat, Leningrad. 242 pp. (in Russian).
- Skipov, V.P., Koverda, V.P., 1984. *Spontaneous Crystallization of Supercooled Liquids*. Nauka, Moscow. 232 pp. (in Russian).
- Smith, R.S., Kay, B.D., 1999. The existence of supercooled liquid water at 150K. *Nature* 398, 788–791.
- van de Hulst, H.C., 1957. *Light Scattering by Small Particles*. John Wiley, New York. 570 pp.
- Volkovitsky, O.A., Pavlova, L.N., Petrushin, A.G., 1984. *Optical Properties of Crystal Clouds*. Gidrometeoizdat, Leningrad. 198 pp. (in Russian).